Quantum Chemical Calculations of the Structures and Electronic Properties of *N,N′*-Bis(3,5-dibromosalicylidene)-1,2-diaminobenzene and Its Cobalt(II) Complex. Origin of the Redox Activity of the Cobalt Complex

G. L. Estiú,[*,†,‡] **A. H. Jubert,**[*,†] **J. Costamagna,**[§] **and J. Vargas**[§]

QUINOR, Departamento de Química, Facultad de Ciencias Exactas, Universidad Nacional de La Plata, CC 962, 1900 La Plata, Argentina, Departamento de Ciencia y Tecnología, Universidad Nacional de Quilmes, Roque Saenz Peña 180, 1876 Bernal, Argentina, and Departamento de Química Aplicada, Facultad de Química y Biología, Universidad de Santiago, Santiago 2, Chile

Coordination transition metal compounds are strongly related to charge transfer mechanisms[1−7] and have gained importance, in the last years, for the study of several biological and catalytic processes, where they serve as synthetic models that compare more or less successfully with the more extended systems. Co complexes with ligands derived from salicylaldimines have been found useful for the catalytic reduction of naphthas.[3] On the basis of the similarity to the redox process involved in vitamin B[12] metabolism,[8] a mechanism has been proposed that involves several steps associated with different oxidation states of the central atom, with an initial stage defined by the reduction of Co(II) to Co(I). The information available on the redox behavior of complexes with acyclic Schiff bases is rather limited, and no theoretical interpretation of the mechanisms involved in the related reactions has been reported to this time.

We report, in this paper, the results of the application of a combination of semiempirical AM1 and INDO calculations to the study of the structural, electronic and spectroscopic properties of *N,N′*-bis(3,5-dibromosalicylidene)-1,2-diaminobenzene

(DBSD) and its cobalt complex,[3,9−15] mainly focusing on the mechanisms involved in the redox activity of the latter. The interpretation of the UV−visible spectra of the isolated ligand, characterized by a keto−amine ⇌ enol−imine equilibrium (Figure 1) and reflected in its bright orange color, has appeared itself as a challenging subject for theoretical calculations, as neither the keto nor the enol form allows us to reproduce the low-energy region of the UV−visible spectrum. Thus, our success in the interpretation of the origin of the bands around 500 nm also offers a test for the credibility of the calculations.

It is our hope that this study sheds some light on the mechanisms associated with the redox capabilities of the DBSD−Co complex and helps with the design of appropriate modifications that might improve this activity.

We initially performed a search of low-lying conformations of the ligand at the self-consistent field level using the AM1 model Hamiltonian, within the AMPAC package,[16] comparing the stability of the isomers involved in the keto−enol tautomerism, including the Zwitterionic structure (Figure 1a). In order to stabilize the latter, we chose to polarize the molecule, in the framework of the AM1 method, by placing a set of ionic charges (sparkles) at its polar ends. The geometry of the ligand was also optimized by means of INDO/1 calculations,[17] comparing the results derived from both approaches. This method was chosen to optimize the geometry of the Co complex, because of the lack of parametrization of the AM1 Hamiltonian for the Co atom.

According to the AM1 calculations, the enol tautomer is about 8 kcal more stable than the keto. INDO/1 calculations, on the other hand, always favor the enol planar structure from either a keto or an enol starting geometry, as a consequence of an overstabilization of hydrogen bonds. According to this result, we based our further analysis on the structures derived from the AM1 calculations. The geometry of the zwitterion is the result of the AM1 optimization with sparkles of the same geometries defined as initial guesses for the keto form. The local charge densities and the interatomic distances are strongly dependent on the position of the sparkles relative to the carbonyl oxygen and the amine nitrogen. We chose the distance on the basis of the best reproduction of the UV−visible spectra, as minimization of the energy will always favor the CO, CN distances closest to those of the more stable keto form. Both INDO/1 and AM1 calculations give a planar structure of C_{2v} symmetry for DBSD tetracoordinated to a central transition metal atom (Figure 1d).

The electronic characteristics of both the ligand and the Co-(II), Co(I) complexes were analyzed at the configuration interaction (CI) level by means of an INDO/S Hamiltonian[17,18] for the most stable structures that result from the geometry

† Universidad Nacional de La Plata.
‡ Universidad Nacional de Quilmes.
§ Universidad de Santiago.
(1) (a) Simon, J.; Andre, J. *J. Molecular Semiconductors*; Springer: Berlin, 1985. (b) Nevin, W. A.; Chamberlain, G. A. *J. Appl. Phys.* **1991,** *69,* 4324. (c) Hoffman, B. M.; Ibers, J. A. *Acc. Chem. Res.* **1983,** *16,* 15. (d) Kobayashi, N.; Janda, P.; Lever, A. B. P. *Inorg. Chem.* **1992,** *31,* 5172. (e) Collman, J. P.; Zhang, X.; Lee, V. J.; Brauman, J. I. *J. Chem. Soc., Chem. Commun.* **1992,** 1647.
(2) (a) Sparks, L. D.; Medforth, C. J.; Park, M. S.; Chamberlain, J. S.; Ondrias, M. R.; Senge, M. O.; Smith, K. M.; Shelnutt, J. A. *J. Am. Chem. Soc.* **1993,** *115,* 581. (b) Furenlid, L. R.; Renner, M. W.; Fajer, J. *J. Am. Chem. Soc.* **1990,** *112,* 8987. (c) Geno, M. K.; Halpern, J. *J. Am. Chem. Soc.* **1987,** *109,* 1238. (d) Alden, R. G.; Ondrias, M. R.; Shelnutt, J. A. *J. Am. Chem. Soc.* **1990,** *112,* 691. (e) Stichternath, A.; Schweitzer-Stennerr, R.; Dreybrodt, W.; Mak, R. S. W.; Li, X.; Sparks, L. D.; Shelnutt, J. A.; Medforth, C. F.; Smith, K. M. *J. Phys. Chem.* **1993,** *97,* 3701.
(3) Costamagna, J.; Vargas, J.; Latorre, R.; Alvarado, A.; Mena, G. *Coord. Chem. Rev.* **1992,** *119,* 67.
(4) Bilsel, O.; Rodriguez, J.; Milam, S. N.; Gorlin, P. A.; Girolami, G.; Suslick, K. S.; Holten, C. *J. Am. Chem. Soc.* **1992,** *114,* 6528.
(5) Barkigia, K. M.; Fajer, J. In *The Photosynthetic Reaction Center*; Deisenhofer, J., Norris, D. J. R., Eds.; Academic Press: San Diego, CA, 1993.
(6) Bixon, M.; Fajer, J.; Feher, G.; Freed, J.; Gamliel, D.; Hoff, A. J.; Levanon, H.; Mobius, K.; Nechustai, R.; Norris, J. R.; Scherz, A.; Sessler, J. L.; Stehlik, D. *Isr. J. Chem.* **1992,** *32,* 369.
(7) Bilsel, O.; Rodriguez, J.; Milam, S. N.; Gorlin, P. A.; Girolami, G. S.; Suslick, K.; Holten, D. *J. Am. Chem. Soc.* **1992,** *114,* 6528.
(8) Glusker, J. P. In *Structural Studies of Molecules of Biological Interest*; Dodson, G., Gluker, J. P., Sayre, D., Eds.; Claredon Press: Oxford, U.K., 1981; Chapter 14.

(9) Araya, L.; Vargas, J.; Costamagna, *J. Transition Met. Chem.* **1986,** *11,* 319.
(10) McCarty, P. J.; Hovey, R. J.; Ueno, K.; Martell, E. *J. Am. Chem. Soc.* **1955,** *77,* 5820.
(11) Costamagna, J.; Araya, L.; Latorre, R. *Pure Appl. Chem.* **1989,** *61,* 829.
(12) Campos, M.; Diaz, G.; Godoy, S.; Aballay, O.; Costamagna, J.; Latorre, R. *Spectrosc. Lett.* **1991,** *24,* 699.
(13) Campos, M.; Figueroa, K.; Latorre, R.; Manriquez, V.; Diaz, G.; Costamagna, J.; Otero, M. *Vib. Spectrosc.* **1992,** *4,* 77.
(14) Campos, M.; Figueroa, K.; Latorre, R.; Diaz, G.; Costamagna, J.; Canales, J.; Rey, M.; Derouault, J. *J. Vib. Spectrosc.* **1993,** *6,* 25.
(15) Lever, A. B. P. *Inorganic Electronic Spectroscopy*, 2nd ed.; Elsevier: New York, 1984.
(16) Liotard, D. A.; Healy, E. F.; Ruiz, J. M.; Dewar, M. J. S. AMPAC, version 2.1. The Dewar Research Group, University of Texas at Austin.
(17) Zerner, M. C. ZINDO Package. Quantum Theory Project, Williamson Hall, University of Florida.
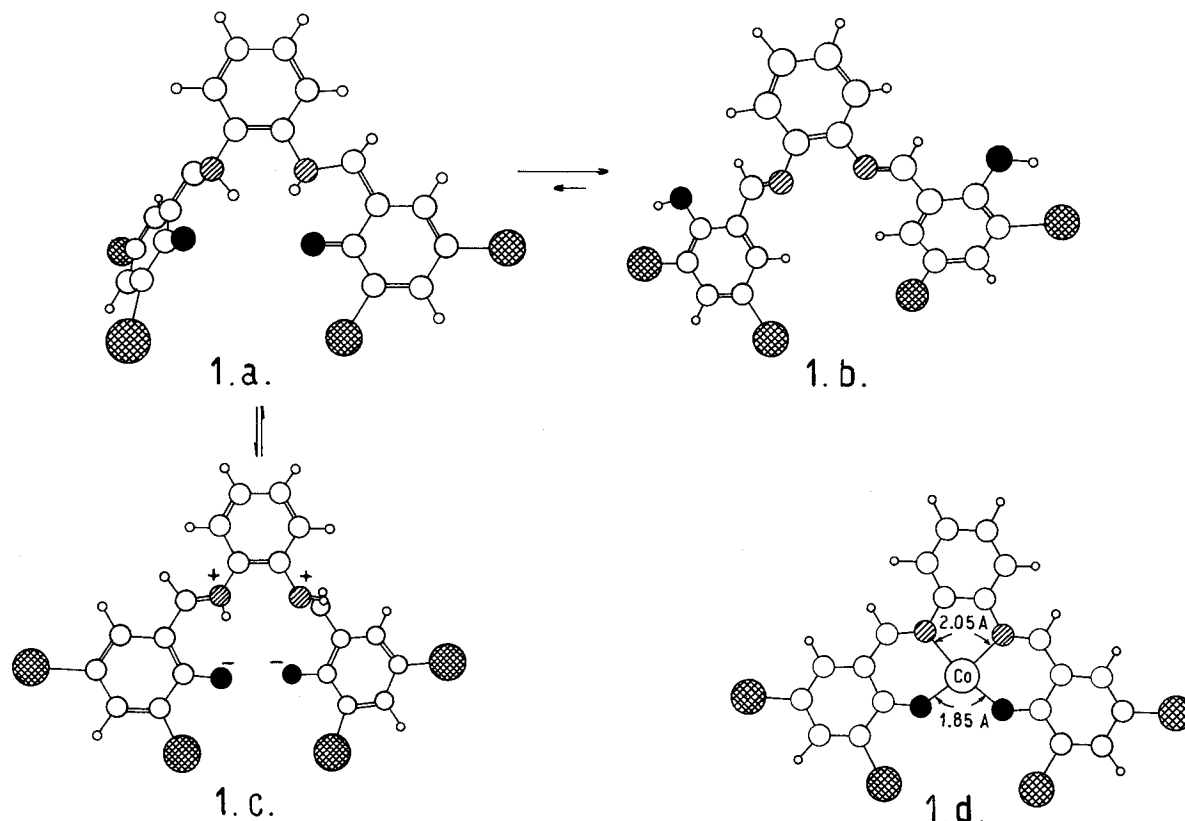
Figure 1. Lowest energy conformations of the keto−amine (a), enol−imine (b), and zwitterion (c) ligand and Co(II) complex (d) structures, as result of AM1 and INDO/1 calculations: cross-hatched circles, Br; solid circles, O; Large open circles, C; striped circles, N; small open circles, H.

Table 1

INDO/S-CI calculated excited states of the keto-amine⌡, enol-imine♦ and zwiterionic⌡⌡ forms of DBSD ligand. (f) oscillator strength

λcalc [nm] (f)	Label	Main Conf. CI coef.	λexp[nm]
⌡403.4 (0.3924)	(HOMO-LUMO). n⇒π*	71⇒72 (-0.795)	380
383.1 (0.0679)	n⇒π*	67⇒72 (0.456)	
367.2 (0.8470)	n⇒π*	70⇒72 (-0.617)	345
287.5 (0.2804)	n⇒π*	70⇒73 (-0.660)	
280.8 (0.0025)	n⇒π*	70⇒72 (-0.505)	
262.8 (0.2014)	π⇒π*	66⇒72 (0.513)	
238.1 (0.2539)	n⇒π*	71⇒80 (-0.509)	
♦332.9 (0.5903)	(HOMO-LUMO).π⇒π*	71⇒72 (-0.888)	
335.5 (0.2980)	π⇒π*	71⇒73 (0.560)	
275.9 (0.2401)	π⇒π*	68⇒72 (0.531)	
258.3 (0.3947)	π⇒π*	67⇒72 (-0.521)	
228.9 (1.3506)	π⇒π*	71⇒79 (-0.422)	
⌡⌡592.7 (0.1532)	(HOMO-LUMO). n⇒π*	71⇒72 (-0.983)	540
488.3 (0.0073)	n⇒π*	69⇒72 (0.877)	
461.6 (0.2716)	(HOMO-3-LUMO+2)n⇒π*	68⇒73 (-0.569)	500
436.1 (0.3004)	(HOMO-3-LUMO+2.n⇒π*	68⇒73 (-0.614)	420
369.9 (0.0087)	n⇒π*	70⇒72 (0.884)	
366.1 (0.0043)	n⇒π*	71⇒73 (-0.918)	
298.8 (0.2766)	π⇒π*	67⇒73 (0.482)	

Table 2

INDO/S-CI calculated states of the DBSD-Co(II) and Co(I) ⇓ complexes. (f) oscillator strength

| λcalc (f) [nm]	Main Conf. CI coef	Sym. State	Label	Pol.	λexp [nm]
3439.0 (0.0000)	a₂ ⇒ a₁ (0.467)	²A₂	$d_{yz}{\Rightarrow}d_{z^2}$		
2136.9 (0.0000)	b₂ ⇒ a₁ (0.817)	²B₂	$d_{xz}{\Rightarrow}d_{z^2}$	y	
903.9 (0.0000)	a₁ ⇒ a₁ (-0.874)	²A₁	$d_{x^2-y^2}{\Rightarrow}d_{z^2}$	z	
736.9 (0.0013)	a₁ ⇒ b₁ (0.908)	²B₁	d⇒π*	x	690
610.4 (0.0000)	b₂ ⇒ a₂ (-0.432)	²B₁	π⇒π*	x	630
580.1 (0.0002)	a₁ ⇒ b₁ (-0.476)	²B₁	d⇒π*	x	590
552.6 (0.0001)	a₁ ⇒ b₁ (-0.705)	²B₂	d⇒π*	y	550
503.7 (0.0003)	a₂ ⇒ b₁ (-0.594)	²B₂	d⇒π*	y	510
445.8 (0.0006)	a₁ ⇒ b₁ (-0.861)	²B₁	d⇒π*	x	460
412.5 (0.2097)	b₂ ⇒ a₂ (0.748)	²B₁	π⇒π*	x	420
389.4 (0.4671)	a₂ ⇒ a₂ (0.435)	²A₁	π⇒π*	z	390
324.8 (0.5440)	b₂ ⇒ a₂ (0.601)	²B₁	π⇒π*	x	330
260.2 (0.9431)	a₂ ⇒ b₂ (-0.556)	²B₁	π⇒π*	x	
⇓2203.6 (0.0000)	a₁ ⇒ b₂ (0.467)	²B₂	d⇒π*	x,y	
1486.8 (0.0001)	a₂ ⇒ b₂ (0.817)	²B₁	d⇒π*	x,y	
1204.1 (0.1662)	a₁ ⇒ b₁ (0.908)	²B₁	d⇒π*	x,y	
1113.6 (0.0126)	a₂ ⇒ a₂ (0.961)	²A₁	d⇒π*	z	
543.2 (0.0406)	b₂ ⇒ b₂ (-0.476)	²A₁	d⇒π*	z	
446.6 (0.0500)	b₂ ⇒ a₂ (-0.325)	²B₁	π⇒π*	x,y	
393.5 (0.0750)	b₂ ⇒ a₂ (0.748)	²B₁	π⇒π*	x,y	
386.8 (0.0750)	a₂ ⇒ b₂ (0.886)	²B₁	π⇒π*	x,y	
374.1 (0.1178)	a₂ ⇒ b₂ (0.446)	²B₁	d⇒π*	x,y	
344.6 (0.2023)	a₂ ⇒ b₂ (-0.550)	²B₁	d⇒π*	x,y	
335.0 (0.2060)	a₂ ⇒a₂ (-0.556)	²A₁	π⇒π*	x,y	
324.7 (0.9453)	b₂ ⇒b₂ (-0.345)	²A₁	π⇒π*	z	

optimizations previously described. The calculated local charge densities on the ligand show the expected distribution on the chemical functions involved. For the Co complexes, on the other hand, the Mulliken population analysis after the CI gives a larger local charge density on the central metal atom in the reduced state (-0.377 for Co(II) vs -0.027 for Co(I)), a fact that may help to explain its larger redox activity compared to that in the oxidized state.

(18) Edwards, M. D.; Zerner, M. C. *Theor. Chim. Acta* **1987**, *72*, 347.
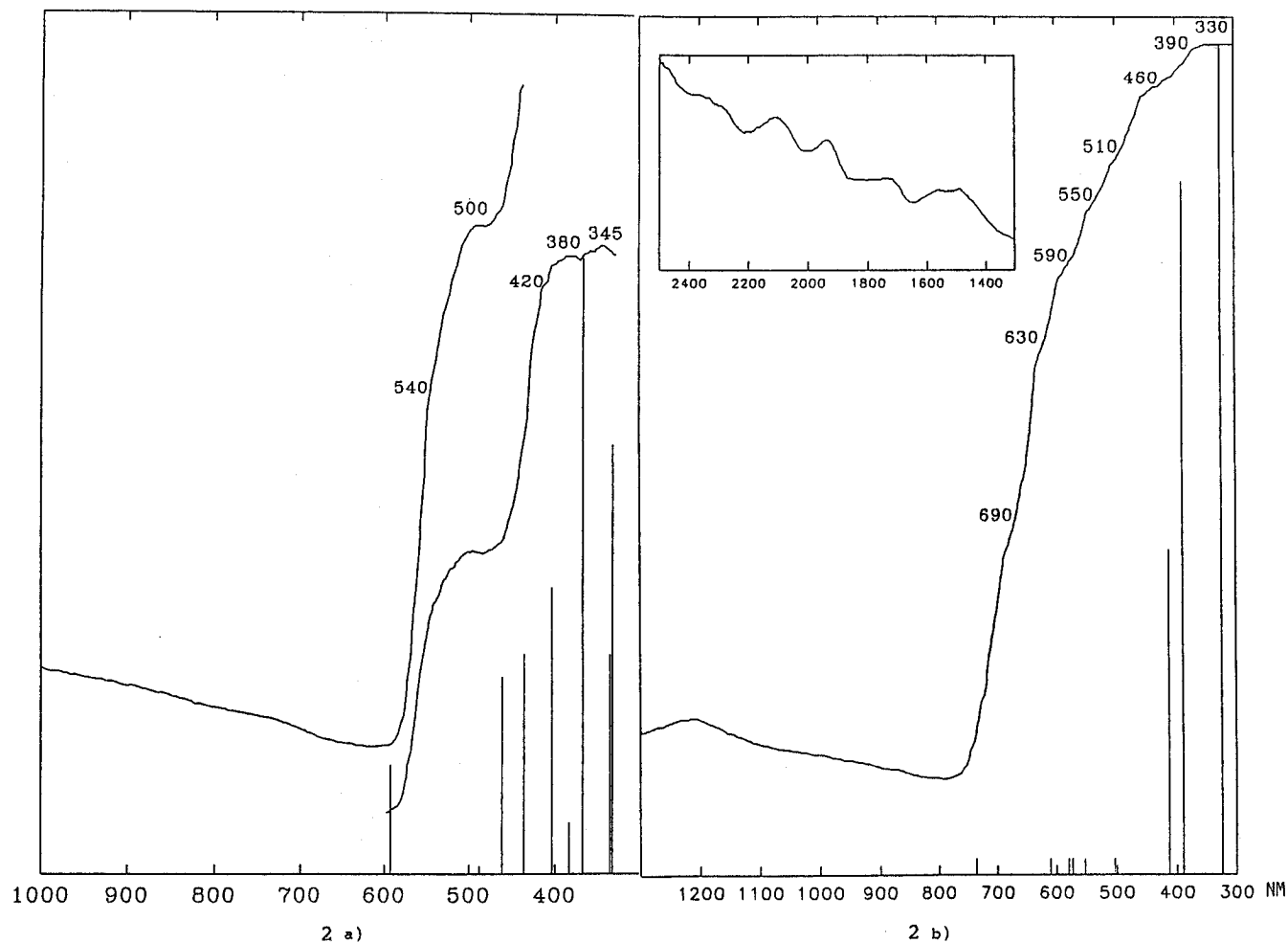
Figure 2. Electronic spectra of DBSD (a) and its Co(II) complex (b). The spectra were recorded on a Karl-Zeiss Model DMR22 instrument. Vertical lines correspond to allowed calculated transitions.

INDO/S-CI calculations have been also performed for the interpretation of the UV−vis spectra (Tables 1 and 2).

The UV−visible spectrum of the ligand (Figure 2) is characterized by low-energy features around 500 nm, which are responsible for its bright orange color. The INDO/S-CIS calculated spectra for the keto and enol forms of DBSD are shown in Table 1.

In the case of the most stable, enol, tautomer, no transition below 332.9 nm is calculated (Table 1). The calculated bands for this tautomer belong, without exception, to $\pi \rightarrow \pi^*$ transitions. For the keto form, on the other hand, $n \rightarrow \pi^*$ transitions involving n electrons localized on the amine nitrogen are calculated at lower energy (Table 1) and allow one to assign the sharp peaks around 400 nm (Figure 2) to these excitations. The shoulder in the low-energy region, around 500 nm, cannot be associated with transitions generated by either the keto or the enol forms. $n \rightarrow \pi^*$ transitions involving electrons on the oxygen atom of the intermediate zwitterionic structure, less tightly bound than that in the carbonyl (keto) structure, are calculated in this region (Table 1).

It is concluded from this analysis, that the simultaneous contributions of all the different conformers, even of the intermediate, less stable one, are required to predict the spectral properties of the ligand. On the other hand, it has to be taken into account that in the solid phase, where the spectra have been determined, the zwitterion-charged structure may be stabilized by mutual electrostatic interactions between the molecular units, becoming closer in energy to the neutral species. Moreover, the observed bands in the low-energy region of the spectra

provide further evidence of the existence of the zwitterionic structure (Figure 1c) in the solid phase.

Calculations for the Co(II) complex show strong d−π mixing, making it difficult to label the orbitals as "d" (centered on the metal) or π (centered on the ligand). There is a major contribution of d $\rightarrow$ d transitions in the low-energy region (Table 2) that is reflected in the local charge density on the central metal atom, which shows no important change after excitation.

The open-shell structure of the Co(II) complex implies a half-filled d_{z^2} HOMO orbital and a completely filled HOMO-1 which is also "d", centered on the metal. The LUMO orbital is, on the other hand, π, centered on the ligand. Low-energy d $\rightarrow$ d locally Lapporte-forbidden transitions belong to excitations filling the hole in the HOMO, whereas the low-energy allowed bands are associated with d $\rightarrow$ π^* charge transfer transitions (Table 2). Higher energy bands are associated with $\pi \rightarrow \pi^*$ transitions, localized on the ligand.

On the basis of experimental evidence,[19] the reducing properties of the salicylidene complexes were associated with the lower oxidation state of the metal center. The redox mechanism implies an initial step when the Co(II) complex is reduced to the Co(I) complex, the latter being the active species for the reduction of naphthas.[20] The analysis of the calculated UV−visible spectra of the reduced complex, together with its electronic properties, can help us to infer whether the activity

(19) Pearce, D. J.; Pletcher, D. *J. Electroanal. Chem. Interfacial Electrochem.* **1986**, *197*, 317.
(20) Collin, J. P.; Sauvage, J. P. *Coord. Chem. Rev.* **1989**, *93*, 245.

is associated with the ligand or with the metal and can provide a further interpretation of the charge transfer mechanism that might be associated with the reactivity. The negative charge density on the central atom of the Co(I) complex shows that the reducing capability is mainly associated with this center. When the UV−vis spectrum is analyzed, the low-energy region is mainly composed of charge transfer d $\rightarrow \pi^*$ transitions that, according to the calculations, would develop at lower energy than for the oxidized Co(II) complex (Table 2). We may infer that a charge transfer from the electron-rich metal center to a ligand bonded to it would be associated with the redox capability. The electron charge density on the metal center decreases markedly for the first excited state, as a consequence of this metal $\rightarrow$ ligand CT. The low energy of the peaks associated with allowed excitations (1204.1 nm) provides further evidence of the reducing properties of the Co(I) complex, which are a consequence of the availability of the d electrons.

IC950219S